Alpha particle dynamics with experimentally reconstructed displacement eigenfunctions in sawtooth oscillations

H. E. Ferrari[1,2], R. Farengo[1], P. L. Garcia-Martinez[2,3], W. Ettoumi[3], M.-C. Firpo[3], A. F. Lifschitz[4]

[1]*Comisión Nacional de Energía Atómica, Centro Atomico Bariloche, Bariloche, Argentina*

[2]*CONICET, Bariloche, Argentina*

[3]*Laboratoire de Physique des Plasmas, Ecole Polytechnique, Palaiseau, France*

[4]*Laboratoire d'Optique Appliquée, ENSTA, Palaiseau, France*

It is generally assumed that sawtooth oscillations will redistribute alpha particles [1]. In particular, ash removal is extremely important in fusion conditions since they could dilute the fuel and consequently terminate the fusion reactions. We study the effect of sawtooth oscillations on alpha particle dynamics. The sawtooth is modeled as in Ref. [2], where the total magnetic field is the sum of a simple analytical equilibrium (large aspect ratio, circular cross section) plus the perturbation produced by the unstable modes. The electric field is obtained from the linear, ideal, Ohm's law $\mathbf{E_1} = -\partial\xi/\partial t \times \mathbf{B}$ including the same modes. The displacement eigenfunctions of the sawtooth ξ^{mn} are reconstructed from experimental measurements [3].

Equilibrium and perturbed fields

The equilibrium magnetic field is obtained by expanding the Grad-Shafranov (GS) equation in powers of the inverse aspect ratio, ε, including only the first two terms in the solution as in Ref. [2]. The q profile and flux surfaces obtained for $\varepsilon = 1/3$, $p_1 = 0.05$ and $B_{pol}(x = 1, \phi = 0) = 0.155$ are shown in Fig. 1 (x is the normalized minor radius and ϕ the poloidal angle). Ideal MHD is used to calculate the perturbed fields produced by a known displacement field

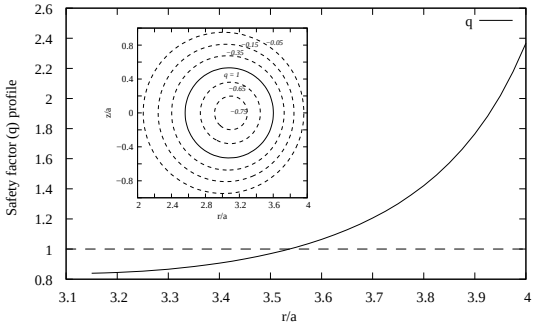

Figure 1: Safety factor and flux surfaces.

$$\mathbf{B}_1 = \nabla \times (\xi \times \mathbf{B}) \qquad \mathbf{E}_1 = -\frac{\mathbf{v}_1 \times \mathbf{B}}{c}, \qquad \mathbf{v}_1 = \frac{\partial \xi}{\partial t}. \tag{1}$$

where E_1 and B_1 are the perturbed electric and magnetic fields, ξ is the displacement and B the equilibrium field calculated above. Following the analysis presented in Refs. [4, 5] we assume

that three modes are present and the x-component of the displacement can be written as

$$\begin{aligned}\xi_x(x,\phi,\theta,t) &= \xi_x^{11}(x) f^{11}(t)\cos(\phi-\theta-\omega t)+\xi_x^{22}(x) f^{22}(t)\cos[2(\phi-\theta-\omega t)]+ \\ &\quad \xi_x^{21}(x) f^{21}(t)\cos(2\phi-\theta-\omega t) \qquad (2)\end{aligned}$$

where θ is the toroidal (azimuthal) angle and ω is the frequency. Considering incompressible displacements ($\nabla\cdot\xi=\mathbf{0}$) and following [6] we can write the other components of ξ in terms of ξ_x. Details of the calculations are presented in Ref. [2].

Results

A fourth order Runge-Kutta method is employed to calculate the exact particle trajectories in the time dependent fields. Collisions are not included because the simulation time is much shorter than the collision time. The time step is taken small enough to guarantee that, when $\mathbf{E}_1$ is not included, the energy and azimuthal (toroidal) component of the canonical momentum (P_θ) are conserved. To study α particle dynamics during sawteeth we consider groups of particles having the same energy distributed according to the plasma density. The initial conditions for each particle are determined using the following procedure: 1) A spatial position is chosen with probability proportional to the plasma density. 2) The energy of the particle is fixed and a random (isotropic) initial direction is chosen. We are interested in comparing the effect of the

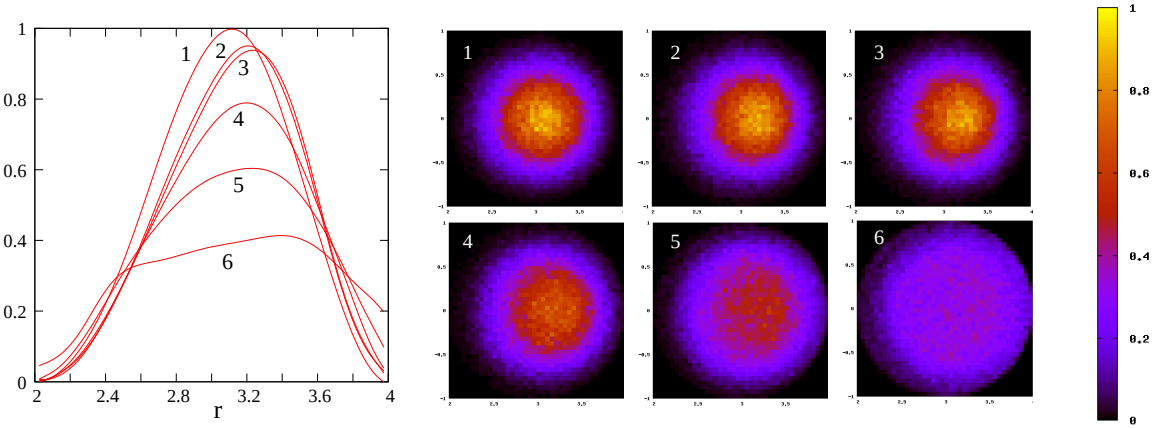

Figure 2: Snapshots of α-particle density evolution.

contribution of the electric field during the crash phase (the electric field can be important if the crash time is short) with that due to the stochasticity of the magnetic field resulting from the introduction of the $(2,1)$ mode. Actually, it is well known that the equations of magnetic field lines can be casted in Hamiltonian form. For tokamaks, the Hamiltonian is the poloidal magnetic flux and reads

$$H(\psi,\theta,\phi)=H_0(\psi)+\sum_{m,n}H_{mn}(\psi)\cos(m\phi-n\theta+\chi_{mn}), \qquad (3)$$

with $H_0(\psi) = \int^{\psi} 1/q(\psi')d\psi'$ and ψ the toroidal magnetic flux conjugated to the poloidal angle ϕ. If one assumes that only $m = n$ modes are present, then the corresponding Hamiltonian (3) can easily be shown to be integrable through a canonical change of variables, with the generating function $F_2(\psi, \theta, \phi) = (\phi - \theta)\psi$, that amounts to moving to the $(1,1)$ wave frame. Introducing a different helicity, here through the $(2,1)$ mode, is required for the magnetic field lines deriving from (3) to become stochastic.

We used TFTR parameters ($B_0 = 5T$, $R_0 = 2.6m$, $a = 0.9m$, $r(q=1) = 0.45m$) and considered 1 MeV α-particles, as in [4]. In Fig. 2 we show density profiles at $z = 0$ (left) and 2D density plots (right) at different times. The snapshots are taken each $\delta t = 0.46$ ms. Curve (1) (and picture (1) on the right) is the initial condition ($t = 0$), (2) is at $t = 0.46$ ms, (3) at $t = 0.93$ ms, and so on. To get a further insight on the role of the different modes and of the electric field, we performed simulations without the mode (2,1) and canceling the electric field. Figure 3(a), shows the time evolution of the maximum α particle density in a sawtooth. Curve (1) is obtained when all the modes are included. Curve (2) is obtained when the electric field is switched off. Curve (3) is obtained when the mode (2,1) is switched off. Curve (4) is $f^{11}(t)$ and curve (5) is $f^{22}(t) = f^{21}(t)$. It is clear that with these parameters, stochastization is more important than the electric field.

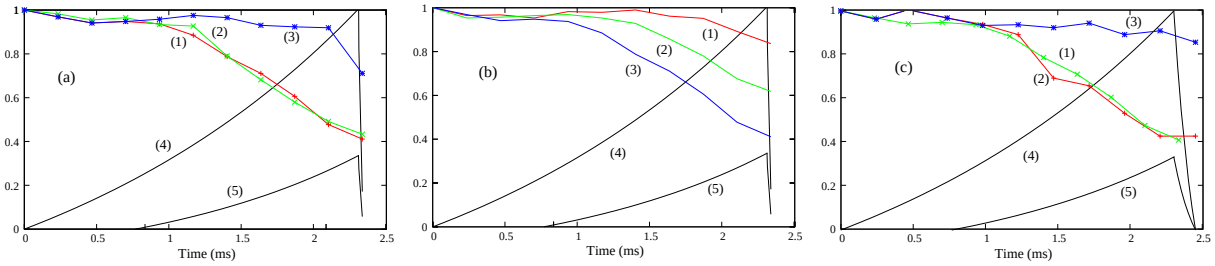

Figure 3: Time evolution of maximum α-particle density.(a) (1) Full simulation. (2) Electric field switched off. (3) mode (2,1) switched off. Curve (4) is $f^{11}(t)$ and curve (5) is $f^{22}(t) = f^{21}(t)$ ($t_{crash} = 15\mu s$). (b) Evolution of the maximum α-particle density for different values of the mode amplitude. (c) Evolution of the maximum α-particle density for different crash times. See the text for references.

In figure 3(b), we show the time evolution of the maximum α particle density for different perturbation amplitudes. Curve (1) is for $\delta B/B = 0.02$, curve (2) is for $\delta B/B = 0.04$ and curve (3) is for $\delta B/B = 0.08$. Curve (4) is $f^{11}(t)$ and curve (5) are $f^{22}(t)$ and $f^{21}(t)$. The change in the maximum density is proportional to the perturbation amplitude. In figure 3(c), we show the time evolution of the maximum α particle density for different crash times. Curve (1) is for $t_c = 15\mu s$, curve (2) is for $t_c = 150\mu s$ and curve (3) is for $t_c = 150\mu s$ and mode (2,1) switched

off. Curve (4) is $f^{11}(t)$ and curve (5) is $f^{22}(t) = f^{21}(t)$ for $t_c = 150\mu s$.

In figure 4 we show the initial and final α-particle distributions at $z = 0$ for passing, co-passing and trapped particles. With the parameters employed all the particles are redistributed

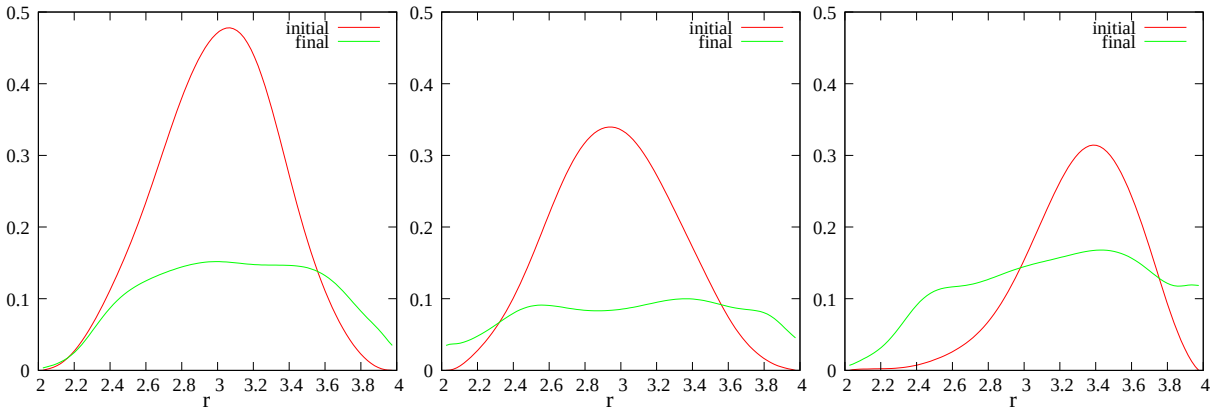

Figure 4: Initial and final α-particle distributions at $z = 0$ at the beginning and at the end of the sawtooth. Left passing particles, middle co-passing particles and right trapped particles.

According to our simulations, stochastization of the magnetic field lines (here due to mode (2,1)) produces a strong redistribution provided that the perturbation is large enough. The crash time, and therefore the electric field, does not play an important role in this regime. This means that a sawtooth model in which only $m = n$ modes are present (as reported in Ref. [5]) will not produce a significant redistribution of the alpha particles. Future studies will be devoted to study the effect of stochastization for ITER like parameters.

Financial support from the ECOS-Mincyt Research Grant No. A09E02 is gratefully acknowledged.

References

[1] A. Fasoli *et al.*, Nuc. Fusion **47**, s246 (2007)

[2] R. Farengo *et al.*, Plasma Phys. Control. Fusion **54**, 025007 (2012)

[3] Ya. I. Kolesnichenko et al., Nucl. Fusion **7**, 1325 (2000)

[4] Y. Zhao and B. White, Phys. Plasmas **4** (4) (1997)

[5] V. Igochine et al., Nuc. Fusion **47**, 23-32 (2007)

[6] J. P. Freidberg, *"Ideal Magneto Hydrodynamics"*, Plenun Press, Chapter 9, (1987)